PRAMANA — journal of physics

Vol. 82, No. 4
April 2014
pp. 659–669

Deformed configurations, band structures and spectroscopic properties of $N = 50$ Ge and Se nuclei

S K GHORUI[1,*] and C R PRAHARAJ[2]

[1]Department of Physics, IIT Ropar, Rupnagar 140 001, India
[2]Institute of Physics, Bhubaneswar 751 005, India
*Corresponding author. E-mail: surja@iitrpr.ac.in

DOI: 10.1007/s12043-014-0714-9; ***e*Publication:** 20 March 2014

Abstract. The deformed configurations and rotational band structures in N=50 Ge and Se nuclei are studied by deformed Hartree–Fock with quadrupole constraint and angular momentum projection. Apart from the 'almost' spherical HF solution, a well-deformed configuration occurs at low excitation. A deformed well-mixed $\Omega = 1/2^+$ neutron orbit comes down in energy (from the shell above $N = 50$) to break the $N = 50$ spherical shell closure. A $K = 7^-$ isomer is predicted in ^{84}Se at fairly low excitation energy. At higher excitation energies (8 MeV), a deformed band with $\Omega = 7/2^+$–$1/2^-$ (based on $h_{11/2}$) neutron 1p–1h excitation, for ^{82}Ge and ^{84}Se, is shown in our calculation. Our study gives insight into possible deformed structures at spherical shell closure.

Keywords. Deformed structure; constrained Hartree–Fock; shell closure; rotational band; electromagnetic properties.

PACS Nos 21.60.–n; 21.10.Ky; 27.50.+e

1. Introduction

The study of nuclei in the vicinity of the most neutron-rich doubly magic nucleus, ^{78}Ni (with $N/Z \approx 1.8$) gained momentum with recent advancements of experimental techniques using radioactive ion beams and fission fragment. Theoretical study of these nuclei provide a challenging testing ground for different models employed to calculate nuclear structure properties. ^{82}Ge and ^{84}Se are nuclei near the neutron drip-line and have been studied in the laboratory in the recent years. Moreover, these two nuclei are likely to occur at the crusts of neutron stars [1]. Considerable experimental and theoretical efforts have been made in this region to study the shell structure of nuclei near the $N = 50$ shell closure (e.g., [2–10] and references therein). The possibility of quenching of the $N = 50$ shell closure has been discussed in [2,5,6,11], while the persistence of the shell closure has also been anticipated in other works [4,8]. Theoretical studies so far have focussed on the $N = 50$ shell closure of these nuclei (or simple particle–hole excitations in spherical

models). No systematic attempt has been made to study the possibility of their deformed structures. True deformation effects can be seen only by considering configuration mixing in a large basis, allowing for excitation across closed shell.

In general, closed shell nuclei exhibit spherical ground state, whereas the breaking of a closed shell can provide coexisting deformed configurations. One of the vital indications of the deformed configurations is the appearance of low-lying excited $K = 0^+$ rotational bands. Collective bands with large deformation have been observed in the doubly magic nuclei, e.g., in ^{16}O ($Z = N = 8$) [12,13] and ^{56}Ni ($Z = N = 28$) [14–16], coexisting with the spherical ground configuration.

Recently, Hwang *et al* [2] have observed deformed rotational bands in ^{82}Ge. To our knowledge, these deformed rotational bands have not been studied theoretically so far though there are attempts to study these nuclei and their neighbours in the various models and approaches including shell model [3,4,9,17,18], microscopic–macroscopic model [19] and self-consistent mean-field models [18,20]. Most of these works, are mainly focussed on the ground state properties of ^{82}Ge, ^{84}Se and their vicinity. In this work, we address the important question of excitation across a major shell by a self-consistent procedure in a deformed basis. A quadropole constraint is used to explore various deformed structures in ^{82}Ge and ^{84}Se.

Here, we study theoretically the low-lying as well as the excited deformed bands and their electromagnetic properties to search for various structures, spherical and deformed, of the exotic nuclei ^{82}Ge and ^{84}Se by employing the deformed Hartree–Fock (HF) and angular momentum (J) projection method [22–24]. Residual interaction is included in self-consistent calculations in building the deformed basis in this theory. From the self-consistent HF calculation one can build the intrinsic states of the bands by particle–hole excitations across the proton and neutron Fermi surfaces (the various particle–hole configurations based on HF intrinsic states), besides the Hartree–Fock configuration. J-projection from the deformed intrinsic configurations gives spectra of various bands [22–24]. Diagonalization after projection can be done. This model, with the residual interaction built into the HF states, is very close to the shell model as has been shown in earlier studies [25–27].

In the §2, we briefly mention the theoretical methods of deformed Hartree–Fock and angular momentum projection. In §3, results for various deformed solutions, obtained with quadrupole constraint, are given. Energy spectra and electromagnetic ($E2$, $M1$) properties obtained by J projection are presented. Section 4 contains the summary.

2. The theoretical method

Here we briefly discuss the deformed Hartree–Fock (with axial symmetry) and angular momentum projection methods. Details of HF theory and equations can be found in refs [21–24]. In the HF theory, the residual interaction is taken into account to obtain the best possible single-particle basis by iteration procedure and the theory is based on variational principle [21,22]. With axial symmetry, a HF single-particle state has good m value and is a superposition of various $|jm\rangle$ states of the shell model basis:

$$|\alpha m\rangle = \sum_j C_j^{\alpha m} |jm\rangle. \tag{1}$$

The mixing amplitudes $C_j^{\alpha m}$ are solved for by HF iteration procedure [21–23].

An HF intrinsic state ($|\phi_K\rangle$), in general, is a superposition of various J-states. The physical states of good J are obtained by angular momentum projection from the intrinsic states. The angular momentum projection operator is

$$P_K^{JM} = \frac{2J+1}{8\pi^2}\int \mathrm{d}\Omega D_K^{JM^*}(\Omega)R(\Omega), \tag{2}$$

where Ω stands for the Euler angles α, β and γ, and $R(\Omega)$ is the rotation operator.

Because of the axial symmetry of the basis states, in the calculation of the matrix elements for the physical quantities, the Euler angles α and γ are integrated out, leaving the Euler angle β for numerical integration.

The Hamiltonian overlap between two states of angular momentum J projected from intrinsic states ϕ_{K_1} and ϕ_{K_2} (axially symmetric basis) is given by [22–24]

$$H^J_{K_1K_2} = \frac{(2J+1)}{2\left(N^J_{K_1K_1}N^J_{K_2K_2}\right)^{1/2}}\int_0^\pi \mathrm{d}\beta\, \sin(\beta) d^J_{K_1K_2}(\beta) \times \langle\phi_{K_1}|H\mathrm{e}^{-i\beta J_y}|\phi_{K_2}\rangle, \tag{3}$$

where $N^J_{K_1K_2}$ are wave function overlaps (integration on Euler angle β of the rotation operator).

$$N^J_{K_1K_2} = \frac{(2J+1)}{2}\int_0^\pi \mathrm{d}\beta\, \sin(\beta) d^J_{K_1K_2}(\beta)\langle\phi_{K_1}|\mathrm{e}^{-i\beta J_y}|\phi_{K_2}\rangle. \tag{4}$$

Reduced matrix element of a tensor operator T^L of polarity L, between projected states $\psi^{J_1}_{K1}$ and $\psi^{J_2}_{K2}$ is given by

$$\left\langle \psi^{J_1}_{K_1} \left\| T^L \right\| \psi^{J_2}_{K_2} \right\rangle = \frac{1}{2}\frac{(2J_2+1)(2J_1+1)^{1/2}}{(N^{J_1}_{K_1K_1}N^{J_2}_{K_2K_2})^{1/2}}\sum_{\mu\nu} C^{J_2LJ_1}_{\mu\nu K_1} \times \int_0^\pi \mathrm{d}\beta\, \sin(\beta) d^{J_2}_{\mu K_2}(\beta)\langle\phi_{K_1}|T^L_\nu \mathrm{e}^{-i\beta J_y}|\phi_{K_2}\rangle. \tag{5}$$

The wave function overlap kernel, the multipole kernels (for $E2$ and $M1$) and the Hamiltonian kernel above are evaluated for various values of angle β and the integration is done numerically, with a large number of Gauss–Legendre points for accuracy. (We use, in this work, 64 G–L points for evaluation and integration of the kernels.)

3. Results and discussion

3.1 *Configurations with constrained HF*

The deformed HF orbits are calculated with a spherical core of ^{56}Ni; the model space spans the $1p_{3/2}$, $0f_{5/2}$, $1p_{1/2}$, $0g_{9/2}$, $0d_{5/2}$, $0g_{7/2}$, $2s_{1/2}$, $0d_{3/2}$ and $0h_{11/2}$ orbits both for protons and neutrons with single-particle energies 0.0, 0.78, 1.08, 3.44, 7.88, 10.47, 11.73, 12.21 and 13.69 MeV, respectively. We use a surface delta interaction [28] (with interaction strength 0.38 MeV for $p-p$, $p-n$ and $n-n$ interactions) as the residual interaction among the active nucleons in these orbits. The shell-model space used in this work is

large enough and adequate to describe the deformation and other properties of nuclei in this mass region. This model space and surface delta interaction give a good description of spectra of nuclei in the $A = 70$–130 region [29]. The interaction matrix elements are reasonable. Comparison of the two-body matrix elements used by us shows closeness, both in sign and magnitude, with the two-body matrix elements of Honma *et al* [9] (in $pfg_{9/2}$ space).

To study the possible structure of the ground band and excited deformed bands of ^{82}Ge and ^{84}Se, we analyse the potential energy surface in HF calculations for various mass-quadrupole moments, $\langle Q_{20}^M \rangle = \langle Q_{20}^p \rangle + \langle Q_{20}^n \rangle$ (with $\langle Q_{20}^p \rangle$ and $\langle Q_{20}^n \rangle$ being quadrupole moments of protons and neutrons, respectively in constrained HF solutions ($\langle\,\rangle$ denotes the HF expectation value)). For constrained HF calculation we use a quadrupole-constrained Hamiltonian given by

$$H'(\lambda) = H - \lambda \left(Q_{20}^p + Q_{20}^n \right), \tag{6}$$

with λ being the constraining parameter. The quadrupole constraint helps to obtain, by self-consistent procedure, the larger deformed solutions; but the Hamiltonian H is used in obtaining energies of various configurations. It is to be noted that $\langle H \rangle$, the original Hamiltonian (and not the constrained Hamiltonian) is used in the evaluation of the energy of the system. The self-consistent energy surface is obtained by plotting $\langle H \rangle$ against deformation parameter β_2 (β_2 is obtained from $\langle Q_{20} \rangle$ for each self-consistent solution). These energy surfaces, for ^{82}Ge and ^{84}Se, are shown in figures 1a and 1b, respectively. At first, an unconstrained HF calculation was done to find the energy minima and shapes of these nuclei. The energy minima from unconstrained calculations are denoted by 'A' and 'B' in figures 1a and 1b, respectively. Then, a constrained HF calculation was performed (by constraining with quadrupole deformation parameter) to find the excited deformed solutions.

In figure 1a, we see that ^{82}Ge exhibits 'almost' spherical (slightly prolate) shape in its ground state. The very weakly deformed prolate (A) and oblate (B) solutions have energy differences less than 1 MeV. Therefore, we took into account the shape mixing of these two configurations after angular momentum projection calculations to obtain the low-lying states. With the constrained calculation, there exists a local minimum (denoted by 'C' in figure 1a) with $\langle Q_{20}^M \rangle \sim 18.0$ (in oscillator length parameter unit) which is shown

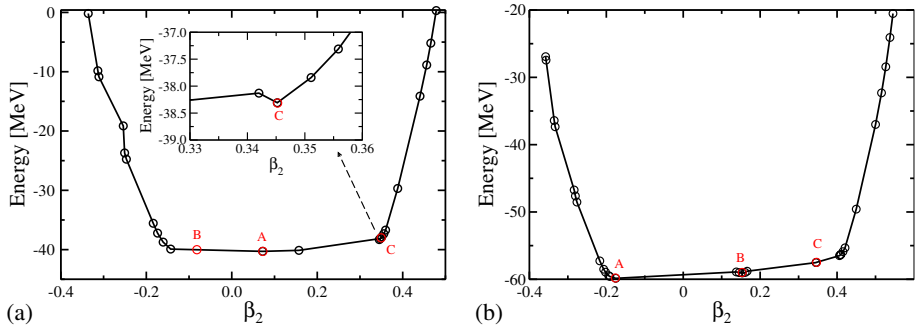

Figure 1. Hartree–Fock energy as function of quadrupole deformation parameter for **(a)** ^{82}Ge and **(b)** ^{84}Se.

in the inset of figure 1a. We get excited rotational bands from this local minimum and from neutron 2p–2h excitation based on this.

In the case of ^{84}Se, from unconstrained HF calculation, we see that the oblate (A) and prolate (B) shapes are nearly degenerate and the oblate shape is energetically lower than the prolate one. To obtain the ground band we have performed the shape-mixing calculation using HF solutions A and B. The deformed bands are obtained by using well-deformed HF solution denoted by 'C' in figure 1b (band D1) and by 2p–2h excitation on the deformed solution C (band D2).

The intrinsic configurations of various excited bands are determined by the orbits near the Fermi surfaces. In figure 2, we show the orbits near the Fermi surfaces for the unconstrained and constrained HF solutions of ^{82}Ge. For the 'almost' spherical solution, the $\nu g_{9/2}$ shell is completely occupied, while for the deformed local minimum C, $\Omega = \pm 9/2^+$ oblate driving neutron orbits are pushed up in energy and are not occupied. The deformed intruder $\pm 1/2^+$ orbits (denoted by '*' in figure 2) from the shell above come sharply down in energy and get occupied.

3.2 *Angular momentum projection results: Energy spectra*

Figure 3 presents the low-lying positive- as well as negative-parity states of ^{82}Ge obtained by angular momentum projection calculations and comparison of experimental data.

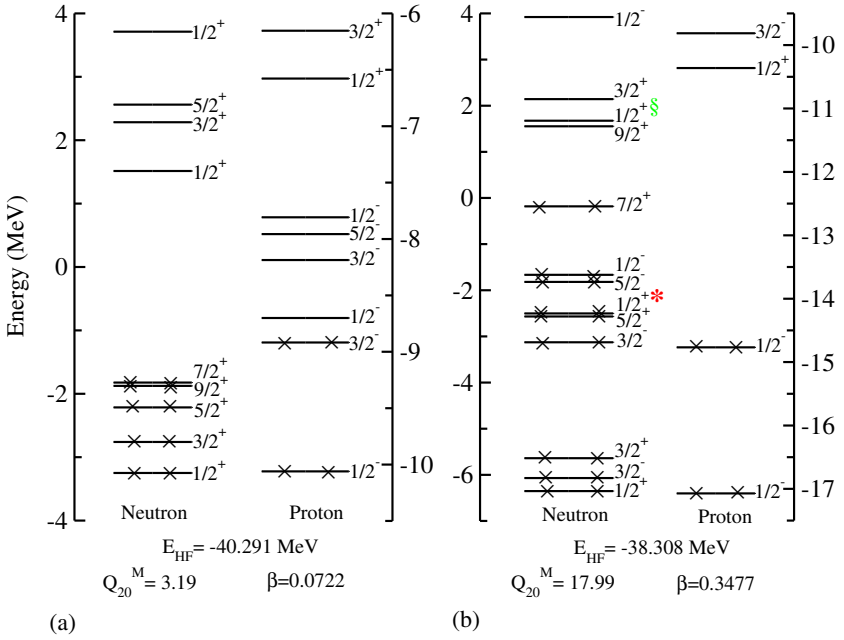

Figure 2. Prolate-deformed HF orbits of ^{82}Ge for (**a**) unconstrained HF (A in figure 1a) and (**b**) constrained HF (C in figure 1a) calculations. HF energy $E_{\rm HF}$ in MeV, mass quadrupole moment $\left(Q_{20}^{M}\right)$ in units of the square of the oscillator length parameter and quadrupole deformation parameter (β) for each solution are shown. The '*' denotes deformed intruder orbit. Only a few levels near the Fermi surfaces are shown.

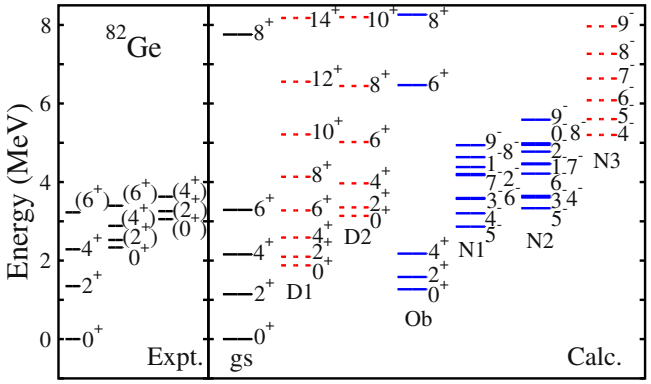

Figure 3. Comparison of experimental spectra (Expt.) and PHF model results (Calc.) for ^{82}Ge. Experimental results are taken from [2,6,31]. Bands obtained with the unconstrained HF calculations are represented as solid lines whereas those obtained from constrained calculations are represented by dotted lines. The notation 'gs' stands for ground state band, 'D1' for deformed 1st excited band and 'D2' for deformed 2nd excited band.

The energy spectra are obtained by free unconstrained (solid lines) and constrained HF (dashed line) calculations. The predicted values are in accord with the experimental results. The predicted 8^+_1 state lies around 4 MeV higher than the 6^+_1 states. Similar results are also obtained by the shell-model calculations of Yoshinaga *et al* [17].

For the recently observed deformed bands, we consider well-deformed constrained HF solutions for this nucleus (figure 2b). Deformation causes migration of prolate deformed levels from the shell above $N = 50$, leading to breaking of the shell gap. This results in strikingly deformed structural properties. The first deformed band (denoted by D1 in figure 3) built on the constrained HF configuration ('C' in figure 1a) has rotational structure. Experimentally, only four levels are known for this band [2]. We obtain a reasonable agreement between the calculated and experimental results. The calculated band head energy is within ∼400 keV of the experiment and the 'moment of inertia' of the band matches quite well. In figure 2b, the $\pm 1/2^+$ orbits below and above the neutron Fermi surfaces are not of pure j-origin, but are well-mixed superpositions of various j-states ($g_{9/2}$, $g_{7/2}$, $d_{5/2}$, $d_{3/2}$ and $s_{1/2}$). We excite two neutrons from the orbits $\pm 7/2^+$ below the neutron Fermi surface to the $\pm 1/2^+$ orbits above to get the second deformed rotational band, D2 of figure 3. A fair agreement between the calculated and the experimental results is achieved. The deformed configuration 'C' has almost no mixing with the configurations 'A' and 'B' (overlaps $H^J_{K_1K_2}$ and $N^J_{K_1K_2}$ of eq. (3) are vanishingly small).

We predict a low-lying positive-parity band ('Ob' in figure 3) based on the oblate unconstrained HF solution 'B'. This oblate HF solution 'B' which was nearly degenerate to the prolate solution 'A' (with energy difference less than 1 MeV) is pushed up in energy (band-head energy ∼1.2 MeV) after angular momentum projection and shape mixing calculations. We also obtain negative-parity bands (N1 and N2 in figure 3) from proton 1p–1h excitation in unconstrained HF solution (prolate). A $K = 4^-$ band (N3 in figure 3) is obtained by 1p–1h excitations across the neutron Fermi surface (constrained HF solution) with dominant configuration $\nu 1/2[301]^{-1} \otimes \nu 9/2[404]^1$.

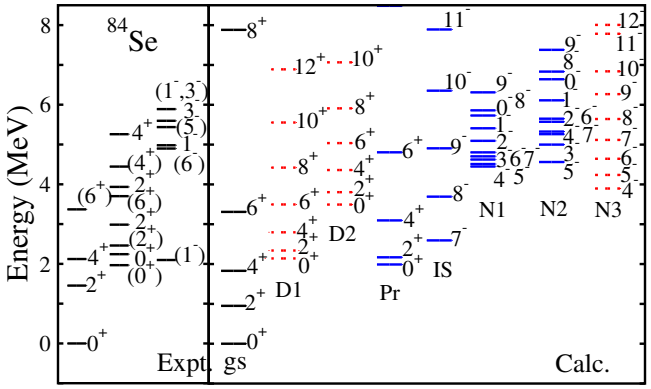

Figure 4. Same as figure 3 but for ^{84}Se. Experimental results are taken from [7,30,31]. We follow the same notation as in figure 3. A band (IS) based on $K = 7^-$ isomer is shown.

About the possible weakening of the $N=50$ shell gap for ^{84}Se, we explore the rotational bands with higher deformation coexisting with the ground band. Experimentally, no deformed rotational band has been seen in ^{84}Se so far. We predict the core excited deformed bands D1 and D2 (dashed line in figure 4) for this nucleus. We also predict a positive-parity band ('Pr' in figure 4) built on prolate HF solution (unconstrained) of ^{84}Se and negative-parity bands (N1 and N2 in figure 4) built by proton excitations from prolate unconstrained HF solution. Using constrained HF solution, we predict a $K = 4^-$ band (N3 in figure 3) built on neutron 1p–1h excitation. A few negative-parity states are experimentally observed in ^{84}Se at energies above 4 MeV. Our calculations for negative-parity states are comparable to the experimental results with the exception of the low-lying 1^- state which is not reproduced.

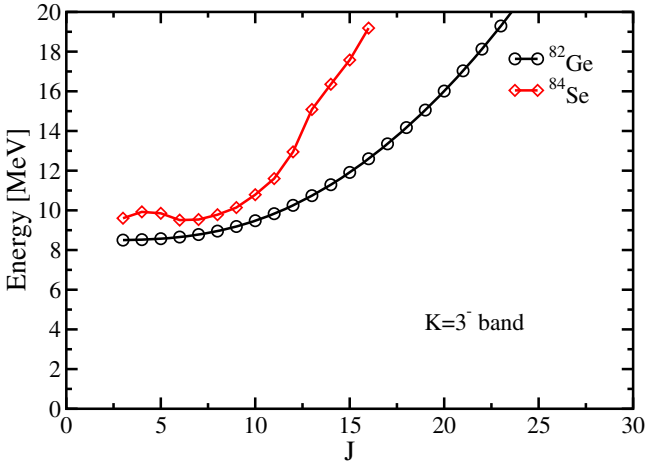

Figure 5. $K = 3^-$ bands for ^{82}Ge (line with circle) and ^{84}Se (line with diamond).

For unconstrained oblate HF solution, the orbits near the proton Fermi surface are based on $\pi f_{5/2}$ and $\pi g_{9/2}$ orbitals with large Ω. These high-j orbits can be coupled to give K-isomers in these nuclei. We predict a low-lying (band-head energy $\approx$2.6 MeV) $K = 7^-$ isomeric band in ^{84}Se (band denoted by 'IS' in figure 4) with the dominant configuration $\pi 5/2[303] \otimes \pi 9/2[404]$.

From the constrained HF solutions of ^{82}Ge and ^{84}Se, we obtain $K = 3^-$ prolate deformed band by exciting a neutron from $\Omega = 7/2^+$ orbit to $\Omega = 1/2^-$ (based on $h_{11/2}$) orbit. These bands are shown in figure 5.

3.3 *Electromagnetic properties*

To check the collectivity of the various bands, we calculate the in-band electric quadrupole reduced transition probabilities $B(E2)$, static quadrupole moments $Q_S(J)$ and magnetic dipole moments $\mu(J)$. The calculated values and available experimental results are shown in table 1. The quadrupole properties are obtained with effective charges of 1.7e and 0.7e

Table 1. Calculated in-band reduced transition moments $B(E2;\ J\rightarrow J-2)$, spectroscopic quadrupole moments $Q_S(J)$ and magnetic dipole moments $\mu(J)$ for ^{82}Ge and ^{84}Se. The short notation gs stands for ground state band, D1 for the 1st deformed band and D2 for the 2nd deformed band. Comparisons with experimental results are made whenever they are available.

Nucleus	J^π	$B(E2;\ J\rightarrow J-2)$ (e^2b^2)		$Q_S(J)$ (eb)	$\mu(J)$ (nm)
		Calc.	Expt. [3]		
^{82}Ge	2^+_{gs}	0.025	0.026±0.004	−0.213	2.135
	4^+_{gs}	0.036		−0.203	3.132
	6^+_{gs}	0.048		−0.218	2.055
	2^+_{D1}	0.170		−0.836	0.839
	4^+_{D1}	0.241		−1.064	1.248
	6^+_{D1}	0.260		−1.168	1.552
	2^+_{D2}	0.192		−0.887	0.715
	4^+_{D2}	0.272		−1.284	1.064
	6^+_{D2}	0.295		−1.240	1.322
^{84}Se	2^+_{gs}	0.022	0.021±0.003	−0.285	1.732
	4^+_{gs}	0.025		−0.314	2.496
	6^+_{gs}	0.021		−0.328	2.884
	2^+_{D1}	0.193		−0.891	0.829
	4^+_{D1}	0.273		−1.133	1.237
	6^+_{D1}	0.297		−1.243	1.544
	2^+_{D2}	0.249		−1.011	0.995
	4^+_{D2}	0.354		−1.287	1.484
	6^+_{D2}	0.384		−1.414	1.854

Table 2. Calculated in-band reduced transition moments $B(E2)$ for $K = 3^-$ band of ^{82}Ge and ^{84}Se. Note the considerable staggering and signature effects in $B(E2)$ values and the signature inversion at higher J.

J^π	$B(E2; J\to J-1)$ (e^2b^2)		J^π	$B(E2; J\to J-2)$ (e^2b^2)	
	^{82}Ge	^{84}Se		^{82}Ge	^{84}Se
4^-	2.804	0.290	5^-	0.819	0.069
5^-	3.225	0.320	6^-	1.721	0.131
6^-	3.192	0.373	7^-	2.592	0.198
7^-	2.919	0.430	8^-	3.418	0.304
8^-	2.695	0.442	9^-	4.199	0.390
9^-	2.484	0.426	10^-	4.938	0.441
10^-	2.297	0.388	11^-	5.634	0.488
11^-	2.130	0.347	12^-	6.291	0.478
12^-	1.983	0.308	13^-	6.902	0.541
13^-	1.852	0.299	14^-	7.475	0.578
14^-	1.734	0.254	15^-	7.996	0.740

for protons and neutrons, respectively. The experimental $B(E2)$ value is known for the lowest $2^+ \to 0^+$ transition for the ground bands [3,4,8]. Our calculated values agree well with the experimental values and also with the shell model calculations of [3,4,9]. To calculate magnetic dipole moments, we use the quenching factor 0.75 of the spin g-factors to take into account the core polarization effect [9] and orbital g-factors are taken as 1.0 for protons and 0.0 for neutrons. Experimental results are not available for magnetic dipole moments; however, our values are consistent with the other calculations in this region [9,32]. The proton contribution is substantially larger than the neutron contribution for the ground band, whereas for the deformed bands the neutron spin contribution dominates over the proton spin contribution, a clear structural change from the spherical ground band to deformed rotational bands, both in deformation and magnetic properties.

For deformed $K = 3^-$ band involving the high-j orbit $h_{11/2}$, the calculated $B(E2)$ values are given in table 2 showing interesting signature effects in the $B(E2)$ values for $J \to J-1$ transitions [33]. There is also signature inversion in $B(E2)$ values at higher spins, as seen in table 2. In the case of ^{82}Ge, the $K = 3^-$ band is considerably more collective compared to the ground and other deformed bands.

4. Summary and concluding remarks

To summarize, we use a self-consistent mean-field model to study the structure of $N = 50$ Ge and Se nuclei with special interest on deformed rotational bands. Constrained Hartree–Fock and angular momentum projection theories for the spectroscopic properties of these two nuclei for various deformations, nearly spherical as well as deformed, are used to obtain the energies and electromgnetic multipole matrix elements of various bands. For each of these two nuclei a unique quantum mechanical energy surface is obtained in axially symmetric quadrupole deformation space by self-consistent constrained Hartree–Fock method. We find low-lying $K = 0^+$ deformed rotational bands

for both the nuclei. These bands are due to the neutron excitations across the $N = 50$ shell from the orbits below the $N = 50$ shell (two and four neutron excitations from $g_{9/2}$). A band based on $K = 7^-$ isomer is predicted in ^{84}Se with the dominant configuration $\pi 5/2[303] \otimes \pi 9/2[404]$. A few levels of the deformed bands have recently been observed in experiment for ^{82}Ge [2] and with the increase of beam intensities, the study of these nuclei will certainly be of more interest. Our present theoretical work throws light on the structures and deformation properties at higher excitation energies in ^{82}Ge and ^{84}Se. We find, at a higher excitation energy, an even more deformed $K = 3^-$ band by excitation of one neutron to $h_{11/2}$ orbit. Thus, this model gives a quantitative and coherent picture of the mechanism for deformation near closed shell and of the band structures of ^{82}Ge and ^{84}Se nuclei and makes some interesting predictions.

As this work shows and the experiment of Hwang *et al* [2] suggests, N=50 Ge and Se nuclei have deformed structures at fairly low excitation energies. Deformed bands are also known to occur in $Z = 50$ Sn nuclei [34] and in other nuclei [35]. Such excited structures at shell closure need thorough theoretical study and experimental study in all regions of nuclei. As the present work shows, a deformed theoretical approach is needed for such studies.

Acknowledgements

The authors thank Prof. R K Bhowmik, Prof. J B Gupta, Dr S Kailas, Dr Z Naik, Prof. S K Patra and Prof. P K Raina for discussions and Prof. A V Ramayya for correspondence. CRP acknowledges the support of the Department of Science and Technology, Govt. of India (DST Project SR/S2/HEP-37/2008) during this work. SKG acknowledges the financial support of the Council for Scientific and Industrial Research (CSIR), Govt. of India (CSIR Project No. 03(1216)/12/EMR II) during this work.

References

[1] G Baym and C Pethick, *Ann. Rev. Nucl. Sci.* **25**, 27 (1975)
[2] J K Hwang, J H Hamilton, A V Ramayya, N T Brewer, Y X Luo, J O Rasmussen and S J Zhu, *Phys. Rev. C* **84**, 024305 (2011)
A V Ramayya *et al*, *Proceedings of 'Frontiers in Gamma-Ray Spectroscopy 2012 (FIG12)'*, New Delhi, to be published
[3] A Gade *et al*, *Phys. Rev. C* **81**, 064326 (2010)
[4] E Padilla-Rodal *et al*, *Phys. Rev. Lett.* **94**, 122501 (2005)
[5] T Rzkaca-Urban, W Urban, J L Durell, A G Smith and I Ahmad, *Phys. Rev. C* **76**, 027302 (2007)
[6] J A Winger *et al*, *Phys. Rev. C* **81**, 044303 (2010)
S Padgett *et al*, *Phys. Rev. C* **82**, 064314 (2010)
[7] A Prévost *et al*, *Eur. Phys. J. A* **22**, 391 (2004)
[8] H Iwasaki *et al*, *Eur. Phys. J. A* **25**, 415 (2005)
[9] M Honma, T Otsuka, T Mizusaki and M Hjorth-Jensen, *Phys. Rev. C* **80**, 064323 (2009)
[10] M-G Porquet and O Sorlin, *Phys. Rev. C* **85**, 014307 (2012)
[11] T Otsuka, T Matsuo and D Abe, *Phys. Rev. Lett.* **97**, 162501 (2006)
[12] E B Carter, G E Mitcheli and R H Davis, *Phys. Rev.* **133**, B1421 (1964)

[13] W H Bassichis and G Ripka, *Phys. Lett.* **15**, 320 (1965)
[14] D Rudolph *et al*, *Phys. Rev. Lett.* **82**, 3763 (1999)
[15] T Mizusaki, T Otsuka, Y Utsuno, M Honma and T Sebe, *Phys. Rev. C* **59**, R1846 (1999)
[16] T Otsuka, M Honma and T Mizusaki, *Phys. Rev. Lett.* **81**, 1588 (1998)
[17] N Yoshinaga, K Higashiyama and P H Regan, *Phys. Rev. C* **78**, 044320 (2008)
[18] K Heyde and J L Wood, *Rev. Mod. Phys.* **83**, 1467 (2011)
[19] P Möller, J R Nix, W D Myers and W J Swiateck, *At. Data Nucl. Data Tables* **59**, 185 (1995)
[20] J-P Delaroche, M Girod, J Libert, H Goutte, S Hilaire, S Péru, N Pillet and G F Bertsch, *Phys. Rev. C* **81**, 014303 (2010)
[21] D J Thouless, *Quantum mechanics of many-body systems* 2nd edn (Academic Press, New York, 1972)
[22] G Ripka, *Advances in nuclear physics* edited by M Baranger and E Vogt (Plenum, 1966), Vol. 1
[23] C R Praharaj, *Structure of atomic nuclei* edited by L Satpathy (Narosa Publication House, New Delhi, 1999), p. 108
[24] C R Praharaj, *J. Phys. G* **14**, 843 (1988); *Phys. Lett. B* **119**, 17(1982); *INT Workshop on Nuclear Many-Body Theories for 21st Century* (University of Washington, 2007)
[25] S B Khadkikar, S C K Nair and S P Pandya, *Phys. Lett. B* **36**, 290 (1971)
[26] S B Khadkikar, D R Kulkarni and S P Pandya, *Pramana – J. Phys.* **2**, 259 (1974)
[27] M H Macfarlane and A P Shukla, *Phys. Lett. B* **35**, 11 (1971)
[28] A Faessler, P Plastino and S A Moszkowski, *Phys. Rev.* **156**, 1064 (1967)
[29] S K Ghorui, P K Raina, A K Singh, P K Rath and C R Praharaj, arXiv:1111.1174v1[nucl-th]
[30] D Abriola *et al*, *Nucl. Data Sheets* **110**, 2815 (2004)
[31] ENSDF database http://www.nndc.bnl.gov/ensdf/
[32] T J Mertzimekis, A E Stuchbery, N Benczer-Koller and M J Taylor, *Phys. Rev. C* **68**, 054304 (2003)
[33] C R Praharaj and A K Rath, *Euro. Phys. Lett.* **7**, 305 (1988)
[34] H Harada *et al*, *Phys. Lett. B* **207**, 17 (1988)
[35] H Mach *et al*, *Phys. Lett. B* **230**, 21 (1989)